PLOS ONE

RESEARCH ARTICLE

Effects of conversion of native cerrado vegetation to pasture on soil hydro-physical properties, evapotranspiration and streamflow on the Amazonian agricultural frontier

Rodolfo L. B. Nóbrega[1]*, Alphonce C. Guzha[1¤], Gilmar N. Torres[2], Kristof Kovacs[1], Gabriele Lamparter[1], Ricardo S. S. Amorim[2], Eduardo Couto[2], Gerhard Gerold[1]

1 Department of Physical Geography, Faculty of Geosciences and Geography, University of Goettingen, Goettingen, Germany, **2** Department of Soil and Agricultural Engineering, Federal University of Mato Grosso, Cuiabá, MT, Brazil

¤ Current address: U.S.D.A. Forest Service, International Programs, c/o CIFOR, World Agroforestry Center, Nairobi, Kenya
* rodolfo.nobrega@geo.uni-gottingen.de

OPEN ACCESS

Citation: Nóbrega RLB, Guzha AC, Torres GN, Kovacs K, Lamparter G, Amorim RSS, et al. (2017) Effects of conversion of native cerrado vegetation to pasture on soil hydro-physical properties, evapotranspiration and streamflow on the Amazonian agricultural frontier. PLoS ONE 12(6): e0179414. https://doi.org/10.1371/journal.pone.0179414

Editor: Julia A. Jones, Oregon State University, UNITED STATES

Received: June 14, 2016

Accepted: May 29, 2017

Published: June 13, 2017

Data Availability Statement: The data of this study is available from the Open Science Framework at osf.io/ubkyd (doi: 10.17605/OSF.IO/UBKYD).

Funding: This research was feasible thanks to the support of the Bundesministerin für Bildung und Forschung (www.bmbf.de) through its grant to GG (CarBioCial project, grant number: 01LL0902A). The authors also acknowledge the financial support of the Fundação de Amparo à Pesquisa do Estado

Abstract

Understanding the impacts of land-use change on landscape-hydrological dynamics is one of the main challenges in the Northern Brazilian Cerrado biome, where the Amazon agricultural frontier is located. Motivated by the gap in literature assessing these impacts, we characterized the soil hydro-physical properties and quantified surface water fluxes from catchments under contrasting land-use in this region. We used data from field measurements in two headwater micro-catchments with similar physical characteristics and different land use, i.e. cerrado sensu stricto vegetation and pasture for extensive cattle ranching. We determined hydraulic and physical properties of the soils, applied ground-based remote sensing techniques to estimate evapotranspiration, and monitored streamflow from October 2012 to September 2014. Our results show significant differences in soil hydro-physical properties between the catchments, with greater bulk density and smaller total porosity in the pasture catchment. We found that evapotranspiration is smaller in the pasture (639 ± 31% mm yr^{-1}) than in the cerrado catchment (1,004 ± 24% mm yr^{-1}), and that streamflow from the pasture catchment is greater with runoff coefficients of 0.40 for the pasture and 0.27 for the cerrado catchment. Overall, our results confirm that conversion of cerrado vegetation to pasture causes soil hydro-physical properties deterioration, reduction in evapotranspiration reduction, and increased streamflow.

Introduction

Despite accounting for nearly half of all tropical forests and approximately 6% of the Earth's land surface, tropical dry forests are underrepresented in the literature on tropical forest

de Mato Grosso (www.fapemat.mt.gov.br; grant number: 335908/2012) and the Brazilian National Council for Scientific and Technological Development (www.cnpq.br; grant number: 481990/2013-5) to RSSA, the German Research Foundation and the Open Access Publication Funds of the Göttingen University to RLBN, and the German Academic Exchange Service (DAAD) and CAPES for the financial support to RLBN and GNT, respectively. The funders had no role in study design, data collection and analysis, decision to publish, or preparation of the manuscript.

Competing interests: The authors have declared that no competing interests exist.

research [1–3]. Further, tropical dry forests are recognized as one of the world's most endangered terrestrial ecosystems, as they are threatened by deforestation and climate change impacts [4].

Available empirical data for tropical forests are insufficient for adequate parameterization of water balance models, including the understanding of the effects of deforestation on evapotranspiration and runoff ratios. Therefore, increased efforts with focus on field-based characterizations and catchment processes are recommended to quantify human influence on all aspects of tropical hydrology [5]. Farrick and Branfireun [3] supported this recommendation, adding that standard hydrological metrics such as runoff coefficients also lack comprehensive characterization in tropical dry forests.

The Cerrado ecosystem, commonly called the Brazilian savanna, is South America's largest tropical dry forest and second-most extensive biome. Although public interest in deforestation in Brazil focuses on the Amazon biome, most of the deforestation has occurred in areas adjacent to the Cerrado-Amazon transition zone [6], also known as the Amazonian agricultural frontier. Approximately 50% of the original 2 million km^2 of the Cerrado area is under agricultural use [7–9], compromising ca. 80% of the primary cerrado vegetation [10]. Other studies indicate that the conversion of cerrado vegetation will continue to be a dominant process of land-use change in Brazil [11,12].

It is widely known that the removal of forest cover associated with agricultural expansion shifts water balances by reducing evapotranspiration and increasing streamflow [13–15]. Studies evaluating the impacts of land-use change on hydrological processes in the Amazon are relatively common [16–21]. However, assessments of the environmental impacts of the Cerrado conversion into agro-pastoral landscapes are scarce [22–24] despite the importance of the cerrado in provisioning and maintaining ecosystem services such as adequate water quantity and quality [25–27]. Although studies show that land-cover change in the Brazilian Cerrado alters the water balance, e.g. by increasing streamflow [28,29], they do not allow generalizations since they are based mostly on low-resolution datasets. In this biome, water balance components such as streamflow and infiltration, and soil physical properties are poorly understood, especially at field scale in the Cerrado [24,30]. Furthermore, the scarcity of hydrometeorological data and the lack of information on vegetation and geological characteristics are major limitations for a reliable quantification of these land-use change effects.

In fact, most of hydrological characterizations of the Cerrado are often limited to either grey or non-peer reviewed literature, which is difficult to access. Evapotranspiration has been the water balance component studied in greater detail in this biome [31,32]. In more recent studies, the emphasis has been on the use of remote sensing techniques to establish a better understanding of evapotranspiration in large areas of the Brazilian Cerrado [33–38]. However, there are limitations to obtain cloud-free satellite images in this region of Brazil [39], and due to inconsistent field information, studies often have restrictions to apply ground-based validation methods [40].

Burt and McDonnell [41] emphasize that there is a noticeable need for field research to seek new fundamental understanding of catchment hydrology particularly in regions outside of the traditional focus, such as the Cerrado. Due to the lack of data with high temporal and spatial resolution for this region of Brazil, macroscale analyses are often the only alternative. Our study focuses on small headwater catchments because they are the origins of larger rivers, and, as outlined by Guzha et al. [42], hydrological signatures exhibited in these catchments can provide useful indicators of environmental changes in larger areas. Studies using small watersheds in the Brazilian Cerrado are usually more feasible than macro-scale approaches to detected hydrological responses to human impacts regarding land-use and land-cover changes [37,43].

Our hypothesis is that conversion of undisturbed cerrado to pasture leads to soil hydro-physical degradation, increased stream discharge, and reduced evapotranspiration fluxes. In this respect, our study aims to aid filling the gap in the understanding of soil degradation and hydrological processes in active deforestation zones on the Amazonian agricultural frontier in Brazil. The specific objectives were to: i) determine soil hydro-physical properties, and; ii) quantify streamflow and evapotranspiration from two adjacent catchments, whose major difference is the land use (undisturbed cerrado vs. pasture).

Methods

Ethics statement

No specific permits were required for our field studies. The accessed areas were privately owned and the respective landowners approved our access during the study period. There was no activity involving sampling or analysis of protected species in our study.

Study area description

We conducted this study in the municipality of Campo Verde (Mato Grosso state, Brazil), situated in the *das Mortes* River basin and in the Cerrado biome (Fig 1). This area is underlain by a Cretaceous sandstone [44]. The soils in this biome are generally highly weathered and acidic

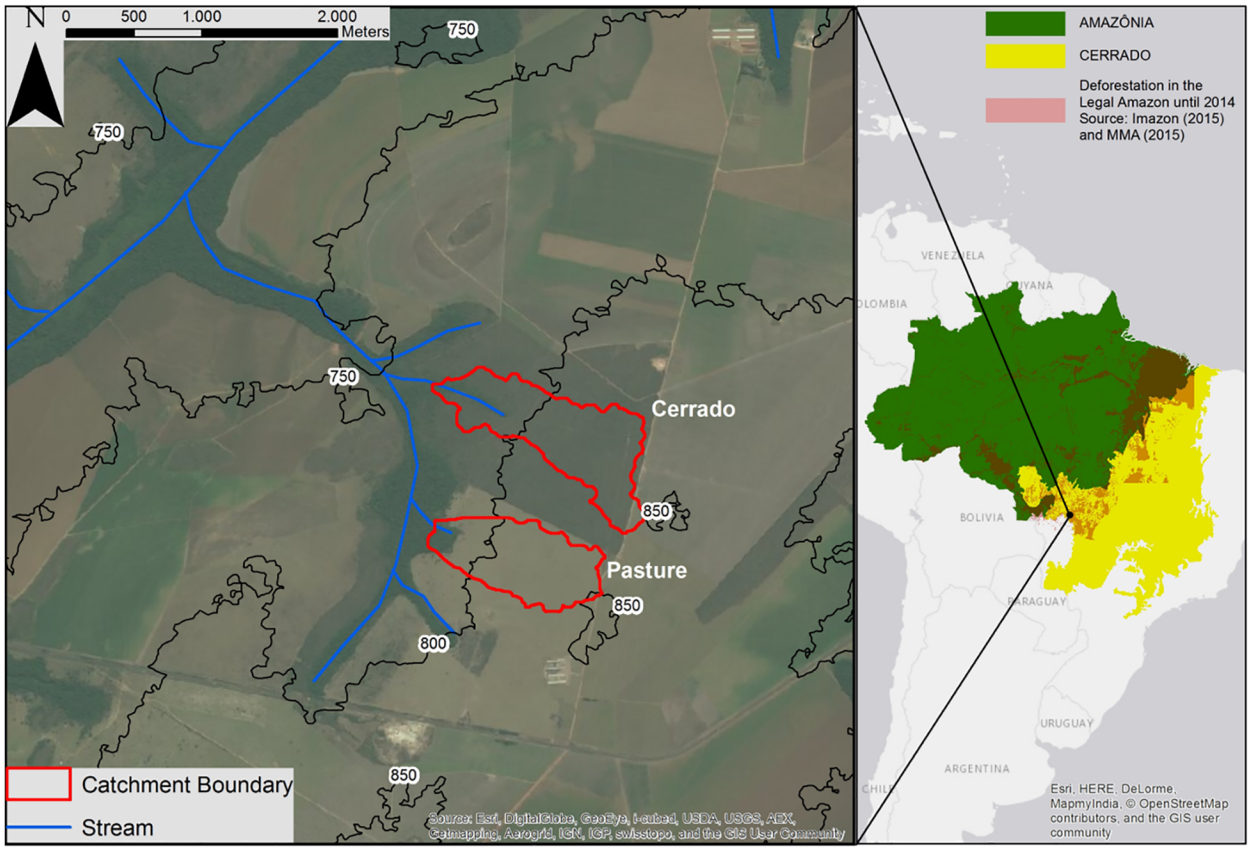

Fig 1. Overview of the Amazon and Cerrado biomes, the deforestation extension in the Legal Amazon, and the location of the cerrado and pasture catchments. Deforestation data from: IMAZON [Internet]; 2016. Available from: http://www.imazongeo.org.br/doc/downloads.php; and MMA [Internet]; 2016. Available from: http://mapas.mma.gov.br/i3geo/datadownload.htm.

https://doi.org/10.1371/journal.pone.0179414.g001

with high aluminum concentrations, thus requiring fertilizers and lime for crop production and livestock farming [45]. The climate in this region is tropical wet and dry, and the mean annual precipitation is 1,800 mm yr^{-1}; the wet season extends from October to April, and the dry season extends from May to September [46].

We compared two adjacent headwater micro-catchments selected on the basis of their Predominant Land Use (PLU), i.e. cerrado vegetation and pasture for extensive cattle ranching, and monitored them from October 2012 to September 2014. The selected catchments are less than 1 km^2 in spatial extent, with similar slopes, aspects, soils, and climate. We used the space for time substitution approach for the comparison between the catchments, which it is often used in hydrology to compare adjacent small catchments with similar characteristics and different land cover [47–51]. This method has yielded significant insights in the hydrologic response of landscapes in the absence of historical data and one major different pattern [52].

With an area of 78 ha, the cerrado catchment is located within the boundaries of the *Rancho do Sol* farm (15.797˚ S, 55.332˚ W) and is mostly covered by cerrado sensu stricto vegetation. The cerrado sensu stricto is described as a deep-rooting and dense orchard-like vegetation consisting of many species of grasses and sedges mixed with a great diversity of forbs, such as *Leguminosae*, *Compositae*, *Myrtaceae*, and *Rubiaceae* plant species, and trees with an average height of 6 m [45,53–56]. The adjacent pasture catchment (58 ha) is located on the *Gianetta* farm (15.805˚S, 55.336˚W). In 1993 the original cerrado vegetation in this catchment was removed and replaced by *Brachiaria* grass species for intensive cattle farming. The soils in both micro-catchments are Arenosols (IUSS Working Group WRB, [57]) characterized by a sandy loam texture, and are correlated with *Entisols Quartzipsamments* (Soil Survey Staff, [58]) and *Neossolos Quartzenicos* (Brazilian Soil Classification, [59]).

Although each catchment was selected on the basis of the PLU, gallery forests exist in both micro-catchments following the stream channel. The width of the gallery forest within each catchment varies from 50 to 200 m. The gallery forests have a higher plant diversity compared to the dominant cerrado vegetation [60,61], and they are common formations in the riparian zones in the Cerrado, which occupy about 5% of the Cerrado biome area [62].

Catchment instrumentation, characterization, and analysis

Topographic survey. To define the catchment boundaries and topographic features for the pasture catchment, we used the Quarryman® Auto-Scanning Laser System (ALS) LaserAce Scanner 300p laser profiling system (Measurement Devices Ltd., UK). Due to interferences of the cerrado vegetation in the laser scanner results, we surveyed the cerrado catchment by using a ProMark™ differential Global Positioning System (dGPS) instrument (Ashtech, USA). For the survey of the gallery forests, we used the dGPS instrument and a Geodetic Rover System (GRS1) GPS (Topcon, USA) with an integrated TruPulse® 360˚ B distance measurement system (Laser Technology Inc., USA). We used the topographic data to develop a Digital Elevation Model (DEM) at 5 m resolution for each catchment. Catchment slope distributions and Compound Topographic Index (CTI) were derived from the DEMs. The CTI is a hydrologically-based compound topographic attribute, represented by a steady state wetness index as a function of both the slope and the upstream contributing area [63]. High CTI is represented by areas with greater contributing areas and low slopes. The CTI was computed using the algorithm described by Gessler et al. [64], which was implemented in ArcGIS® by Evans et al. [65].

Soil geostatistical analysis and sampling. We delineated transects for soil sampling based on the surface elevation and geostatistical analysis of the clay content to regionalize the soil properties [66–68]. For the surface elevation analysis, we used the DEMs derived from the topographic survey, and for the clay content we collected and analyzed 45 disturbed soil

samples at the depth intervals of 0–20 and 40–60 cm from randomly selected points throughout each catchment. We interpolated the clay content results at each soil depth using isotropic variogram analyses and the ordinary kriging method. The variogram results of soil properties as a prerequisite to kriging allow the quantification of the semivariance for any given distance [69].

For the transect delineation only the interpolation of the clay content at 0–20 cm soil depth was used because it showed variogram correlations of 0.94 for the cerrado catchment and 0.83 for the pasture catchment, which were higher than the correlations obtained with the 40–60 cm soil depth. We validated the interpolation results by using the leave-one-out cross-validation method [70], which was based on leaving actual data out one at time and estimating the properties of the location from the neighboring data. We then categorized the surface elevation in 5 equal intervals and clay content in quintiles, and delineated transects from the catchments crest to the stream valley passing over all elevation and clay content categories. We established 15 approximately equally-spaced points along the transects in each catchment to collect in each point one disturbed sample and two undisturbed soil core samples (4.8 cm in diameter and 5.2 cm in height) at depth intervals of 0–10, 10–20, 20–40, and 40–60 cm.

Soil physical and hydraulic properties. The disturbed soil samples were analyzed to obtain the particle size distribution, and the undisturbed samples were used to determine bulk density, saturated hydraulic conductivity (K_{sat}), particle size distribution, total porosity, macroporosity, microporosity, and field capacity. Particle size distributions of the soils were obtained by using the pipette method [71] after chemical dispersion and removal of organic matter and carbonates. Soil bulk density was estimated by weighing the samples after drying them in an oven at 105˚C [72]. K_{sat} was determined by using the constant-head permeameter method. Total porosity was quantified with the cylinder volume method [73]; the macroporosity (pore diameter $\geq$ 0.05 mm) was determined using the tension table method [73]; and the microporosity was obtained by the difference between the total porosity and the macroporosity. Field capacity moisture content was estimated with the pressure membrane method at -0.01 MPa [74].

Rainfall and evapotranspiration. To account for rainfall spatial variability, three tipping bucket rain gauges (0.2 mm resolution) with data loggers (Tinytag®, Gemini, UK) were installed in each catchment to record rainfall at 10-min intervals. A WS-GP1 weather station (Delta-T, UK) installed at a farm approximately 7 km from the two catchments (15.741435˚S, 55.363134˚W) provided total solar radiation, net solar radiation, temperature, relative humidity, wind speed and direction, and rainfall data at 10-min intervals. Using this weather data we quantified the reference evapotranspiration (E_{To}) using the standardized reference evapotranspiration equation [75]:

$$E_{To} = \frac{0.408\Delta(R_n - G) + \gamma \frac{C_n}{T+273} u_2 (e_s - e_a)}{\Delta + \gamma(1 + C_d u_2)}, \quad (1)$$

where E_{To} is in mm day^{-1} or mm h^{-1} for daily or hourly time steps), R_n is the surface net radiation (MJ m^{-2} day^{-1} or MJ m^{-2} h^{-1} for daily or hourly time steps), G is the soil heat flux density (MJ m^{-2} day^{-1} or MJ m^{-2} h^{-1} for daily or hourly time steps), T is the mean daily air temperature (˚C) and u_2 is the wind speed (m s^{-1}) at 2 m height, e_s and e_a are, respectively, the saturation and actual vapor pressure (kPa), $e_s - e_a$ is the saturation vapor pressure deficit (kPa), Δ is the slope of vapor pressure curve (kPa ˚C^{-1}), γ is the psychrometric constant (kPa ˚C^{-1}), C_n and C_d are, respectively, the numerator and denominator constants for the reference type and calculation time step given by ASCE-EWRI [75].

We applied satellite-based image-processing models to improve our E_T estimation for the study area. We estimated the evapotranspiration (E_T) by using a combination of the Surface

Energy Balance Algorithm for Land (SEBAL) and Mapping EvapoTranspiration at high Resolution with Internalized Calibration (METRIC™) models, as described by Allen et al. [76]. Both models are based on the energy balance at the land surface. SEBAL is based on latent heat flux as a residual of the energy balance equation, and its principles and computational basis are described in Bastiaanssen et al. [77] and Bastiaanssen [78]. METRIC considers soil and vegetation as a sole source in the estimation of E_T, and its principles and application procedures are described in Allen et al. [79]. The application of SEBAL has shown to be adequate to quantify the energy balance for the E_T estimation for Cerrado landscapes [40,80], and the use of the METRIC model allows to directly integrate a variety of factors, such as orchard architecture, land-use practices, water stress occurrence, and changes in the weather conditions during the day [81,82].

SEBAL was applied by using a composite of spectral bands 1–7 (path 226 and row 071) of all 13 valid satellite scenes from the Landsat 7 Enhanced Thematic Mapper Plus (ETM+) for our study area and period to determine the energy consumed by the E_T process; this is calculated as a residual of the surface energy equation (Eq (2)) using the software ERDAS Imagine® v. 14 (Hexagon AB, USA). To match the satellite spatial extension, we used a 90-m-resolution DEM (Shuttle Radar Topography Mission, version 4.1, [83]) cropped to the study area to adjust the surface temperature according to the differences in elevation and to derive surface slope and aspect information as required in SEBAL to estimate solar radiation [79]. The Earth-Sun distance parameter, also required by SEBAL, was obtained from Chander et al. [84] when not available in the satellite metadata file.

$$LE = R_n - G - H, \tag{2}$$

where LE is the latent heat flux, R_n is the instantaneous net radiation, G is the soil heat flux, and H is the sensible heat flux (all in W m^{-2}).

METRIC was used to compute the instantaneous E_T from the obtained latent heat flux from SEBAL for each pixel within the catchments at the instant of satellite overpass (Eq (3)). We used two anchor points to define the limit conditions by means of a cold pixel (15.7402˚ S, 55.5292˚ W) and a hot pixel (15.7264˚ S, 55.3325˚ W) for the energy balance over the study area for the internal calibration of sensible heat flux of METRIC [79].

$$E_{Tinst} = 3600\frac{LE}{\lambda\rho_w}, \tag{3}$$

where E_{Tinst} is the instantaneous E_T (mm h^{-1}), 3600 is the time conversion from seconds to hours, ρ_w is the density of water (~ 1000 kg m^{-3}), and λ is the latent heat of vaporization (J kg^{-1}) representing the heat absorbed when one kg of water evaporates and it is computed as:

$$\lambda = [2.501 - 0.00236(T_s - 273.15)] \times 10^6, \tag{4}$$

where T_s is the surface temperature (K).

We applied the evaporative fraction (E_{TrF}) and daily E_{To} to estimate the actual daily E_T assuming that the E_{TrF} is constant during a day [79] according to Eq (5). Additionally, the Penman–Monteith equation, which we used to estimate E_{To}, is known to well-represent the impacts of advection [76]. The E_T values for each type of land use were area-weighted and summed to obtain the total actual evapotranspiration estimation for each catchment.

$$E_T = E_{TrF}E_{To}. \tag{5}$$

The E_{TrF} is calculated as the ratio of the E_{Tinst} derived for each pixel to the E_{To} at an hourly time step computed from weather data at the time of the satellite overpass [76,85] using Eq (6).

Table 1. Satellite scenes description, weather data at the satellite overpass time, and E_{TrF} values.

Landsat 7 ETM+ scene description				Weather station				ETrF			
Date	Satellite overpass time (GMT)	Relative Earth-Sun distance[a]	Solar zenith angle cosine[b]	Air temperature (˚C)	Relative humidity (%)	Wind speed (m s^{-1})	Surface net radiation (MJ m^{-2} h^{-1})	Cerrado		Pasture	
								GF	PLU	GF	PLU
09 Oct 12	13:41	0.99861	0.882	29.5	49%	3.2	612	1.09	0.93	1.25	0.72
02 Mar 13	13:41	0.99108	0.832	26.2	75%	4.6	532	1.21	0.92	1.07	0.64
08 Jul 13	13:41	1.01668	0.652	29.0	34%	2.8	648	0.63	0.52	0.66	0.16
10 Sep 13	13:41	1.00698	0.811	30.9	30%	5.3	558	0.61	0.37	0.70	0.19
26 Sep 13	13:41	1.00250	0.855	27.7	28%	1.9	601	0.84	0.52	0.77	0.15
13 Nov 13	13:41	0.98961	0.905	27.0	66%	3.4	672	1.10	0.76	1.17	N/A[c]
29 Nov 13	13:41	0.98641	0.896	27.9	68%	2.1	667	N/A[c]	1.29	N/A[c]	0.97
01 Feb 14	13:42	0.98536	0.847	27.0	69%	2.9	495	N/A[c]	1.19	N/A[c]	0.51
06 Apr 14	13:42	1.00069	0.791	27.4	73%	2.1	630	1.14	0.96	0.94	0.60
25 Jun 14	13:43	1.01647	0.651	24.5	67%	2.1	430	1.20	0.98	0.96	0.47
11 Jul 14	13:43	1.01661	0.659	20.9	80%	3.4	453	1.20	0.96	1.10	0.45
12 Aug 14	13:43	1.01332	0.725	27.3	46%	2.0	510	0.91	0.68	0.77	0.30
13 Set 14	13:43	1.00620	0.823	30.2	38%	1.8	458	1.16	0.89	1.03	0.61

GF = Gallery Forest area, PLU = Predominant Land Use area

[a] Inverse square and dimensionless.

[b] Dimensionless.

[c] Not available due to cloud masking or Scan Line Corrector-Off malfunction.

https://doi.org/10.1371/journal.pone.0179414.t001

To quantify the E_T we used the mean and the respective ±1 standard deviation of the obtained values for E_{TrF} for the wet and dry seasons, separately, considering all valid pixels within each catchment domain. Table 1 shows the description of the satellite scenes, the main local weather data at the satellite overpass time, and the respective E_{TrF} values for the study areas. Some results were not available due to cloud masking or Scan Line Corrector-Off malfunction [86].

$$E_{TrF} = \frac{ET_{inst}}{E_{To}}. \quad (6)$$

Catchment discharge and hydrograph analysis. At the outlet of each catchment, an adjustable weir was installed. During the wet season the weirs were maintained as rectangular weirs, and during the dry season a v-notch contraction was inserted. At a distance of 2 m upstream of each weir, a DS 5X (OTT, USA) multiparameter probe was installed to measure, among other variables, the water level at 10-min intervals. For the rectangular weir, we used the standard flow equation (Eq (7)) based on the Bernoulli equation to quantify stream discharge. For the v-notch weir, the Kindsvater–Shen equation (Eq (8)) and respective calibration adjustment functions (Eqs (9) and (10)) were used to quantify discharge:

$$Q = \frac{2}{3} C_{dr} b \sqrt{2g} h^{\frac{3}{2}}, \tag{7}$$

$$Q = \frac{8}{15} C_e \sqrt{2g} \tan\left(\frac{\theta}{2}\right) h_e^{\frac{5}{2}}, \tag{8}$$

$$K_h = 0.001[\theta(1.395\theta - 4.296) + 4.135], \tag{9}$$

$$C_e = \theta(0.02286\theta - 0.05734) + 0.6115, \tag{10}$$

where Q is the discharge over the weir ($m^3 s^{-1}$), C_{dr} and C_e are the effective dimensionless discharge coefficients for the rectangular and v-notch weirs, respectively, b is the weir length (m), θ is the v-notch's angle (radians), h is the upstream head above the weir's crest (m), h_e is the effective head ($h + K_h$), and K_h is the head-adjustment factor.

In each catchment, we conducted discharge calibration measurements with an acoustic digital current meter (ADC, OTT, USA) to estimate the C_{dr} factor for each catchment. The obtained C_{dr} values were 0.74 for the cerrado catchment and 0.65 for the pasture catchment. The discharged data were normalized by the correspondent catchment area to allow comparisons between the catchments. To estimate the total streamflow, we used the mean discharge values for each wet and dry seasons. Additionally, we applied ±1 standard deviation of the mean of each wet and dry seasons to the discharge-gap days in order to estimate the total error.

The discharge time series were analyzed with the recursive digital filter method [87] implemented in the Web GIS-based Hydrograph Analysis Tool (WHAT) for baseflow separation [88,89]. The baseflow index (BFI) was computed as the ratio of baseflow to total discharge. The runoff coefficient (R_C) was determined as the ratio of total discharge to total rainfall. Flow-duration curves (FDCs) were derived from the daily discharge data in order to compare the differences in high, low, and median flows between the catchments [90], and catchment flashiness indices were obtained using the method described by Baker et al. [91].

Statistical analyses. Pearson's correlation analysis was applied to test the relationships between the soil properties, and between the rainfall daily values in each catchment. The results were compared using two sample t-test for the data with normal distribution (soil properties), and a nonparametric test (Mann-Whitney U) in the other cases (rainfall, E_T, and streamflow), to determine whether the results were significantly different. The significance threshold was set at .05.

Results

Catchment physiographic attributes

The soil sampling points, the slope distribution, and the CTI for each catchment are shown in Fig 2. The cerrado and pasture catchments have similar slope ranges with most of the values

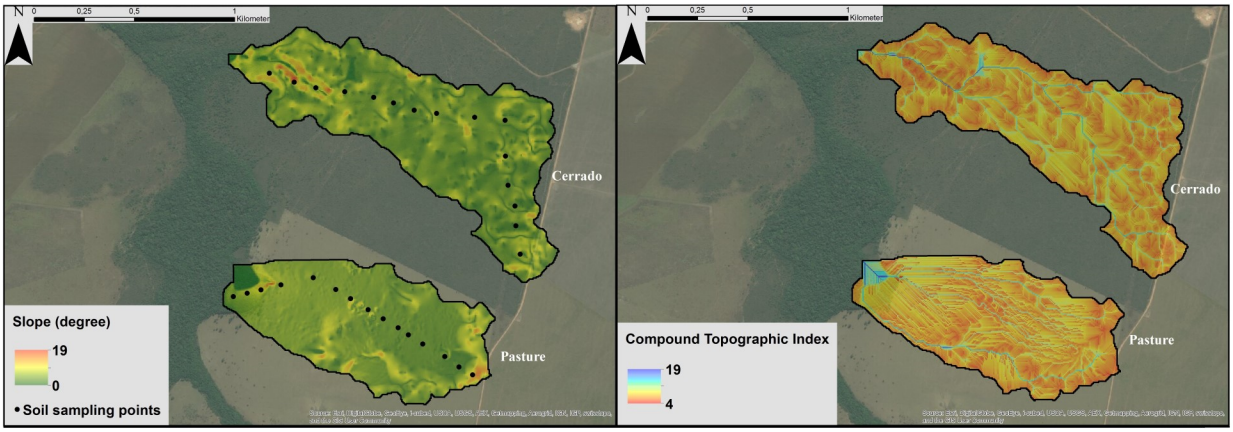

Fig 2. Slope, soil sampling points, and Compound Topographic Index (CTI) in the cerrado and pasture catchments.

https://doi.org/10.1371/journal.pone.0179414.g002

between 0 and 10˚ and an average of approximately 8˚. In both catchments over 95% of the area shows CTI values ranging between 5 and 12, and areas with CTI over 10 have linear form extending from the crest to the outlet of the catchments, which indicates the surface flow pathways.

Table 2 shows a summary of the topographic characteristics of the catchments. The data are distinguished for the gallery forest and the PLU areas. The topographic survey shows that the gallery forests cover approximately 7% of the total areas in both catchments.

Soil physical and hydraulic properties

Table 3 shows that the cerrado and pasture catchments have comparable soil properties. The pasture catchment shows a greater bulk density ($p < .0001$) at 0–40 cm depth and a lower total porosity ($p \approx .0001$) at 0–10 cm soil depth compared to the cerrado catchment. Our findings confirm results from Valpassos et al. [92], who reported greater bulk densities in the topsoil of a pasture compared to an area covered by cerrado vegetation. The gallery forest and the PLU areas of the cerrado catchment do not show significant differences in total porosity and bulk densities with identical bulk density results at 0–10 cm soil depth (1.43 ± 9% g cm^{-3}), whereas these properties found in the gallery forest area of the pasture catchment are significantly smaller than those in its PLU area ($p < .0001$), especially at 0–20 cm soil depth.

Fig 3 shows the relationship between the soil properties in the gallery forest (upper panel) and PLU (lower panel) areas in the cerrado and pasture catchments. As expected, in both catchments the total porosity inversely correlates with the bulk density, and a high correlation

Table 2. Summary of catchments' physical and topographic characteristics.

	Cerrado catchment			Pasture catchment		
	Gallery Forest	**PLU Area**	**Total Area**	**Gallery Forest**	**PLU Area**	**Total Area**
Area (km^2) (% of total)	0.05 (6.4%)	0.73 (93.6%)	0.78 (100%)	0.04 (6.9%)	0.54 (93.1%)	0.58 (100%)
Predominant land cover	Cerrado sensu stricto vegetation			Grassland (*Brachiaria* species)		
Soil type	Arenosols			Arenosols		
Soil texture	Sandy loam			Sandy loam		
Aspect	E-W			E-W		
Average Elevation (m)	770	814	811	775	821	818
Average slope (˚)	7.6	4.6	4.8	3.9	4.4	4.4

https://doi.org/10.1371/journal.pone.0179414.t002

Table 3. Summary of the soil properties.

Catchment	Depth interval (cm)	BD (g cm^{-3})	TP (%)	MaP (%)	MiP (%)	FC (%)	K_{sat} (mm h^{-1})	Sand (%)	Silt (%)	Clay (%)
	0–10	1.43 ± 9% (1.43 ± 9%)	49.2 ± 8% (49.4 ± 10%)	31.8 ± 12% (26.9 ± 13%)	17.4 ± 35% (22.5 ± 36%)	15.9 ± 36% (20.5 ± 40%)	559.5 ± 38% (361.1 ± 15%)	85.8 ± 10% (83.7 ± 8%)	2.4 ± 95% (2.64 ± 109%)	11.9 ± 54% (13.6 ± 27%)
Cerrado	10–20	1.47 ± 6% (1.55)	45.8 ± 5% (45.7)	30.8 ± 18% (28.3)	15.0 ± 32% (17.5)	13.2 ± 37% (16.1)	611.7 ± 45% (363.4)	88.9 ± 2% (81.3 ± 9%)	1.5 ±75% (3.73 ± 78%)	9.6 ± 10% (15.0 ± 29%)
	20–40	1.52 ± 4%	42.9 ± 7%	27.0 ± 18%	15.9 ± 32%	14.7 ± 32%	515.56 ± 56%	87.4 ± 1%	1.3 ± 37%	11.3 ± 7%
	40–60	1.51 ± 3%	42.1 ± 2%	25.2 ± 24%	16.9 ± 36%	15.6 ± 36%	509.6 ± 33%	86.2 ± 1%	1.9 ± 49%	11.9 ± 10%
	0–10	1.56 ± 3% (1.23 ± 10%)	44.4 ± 3% (53.5 ± 4%)	28.1 ± 8% (33.0 ± 9%)	16.4 ± 10% (20.4 ± 16%)	15.5 ± 10% (19.3 ± 19%)	399.0 ± 40% (297.3 ± 52%)	88.4 ± 1% (86.0 ± 2%)	1.5 ± 40% (2.1 ± 8%)	10.1 ± 9% (11.9 ± 12%)
Pasture	10–20	1.57 ± 3% (1.37 ± 3%)	45.7 ± 3% (49.8 ± 5%)	32.1 ± 5% (32.0 ± 10%)	13.6 ± 10% (17.8 ± 9%)	12.9 ± 9% (16.6 ± 13%)	655.6 ± 15% (666.5 ± 46%)	89.2 ± 1% (86.6 ± 2%)	0.9 ± 97% (2.1 ± 48%)	9.9 ± 10% (11.3 ± 22%)
	20–40	1.56 ± 3% (1.41 ± 3%)	46.4 ± 4% (50.3 ± 1%)	32.9 ± 7% (33.6 ± 7%)	13.5 ± 10% (16.7 ± 16%)	12.8 ± 10% (15.8 ± 18%)	705.1 ± 17% (611.3 ± 25%)	87.8 ± 1% (86.7 ± 2%)	1.7 ± 28% (1.9 ± 27%)	10.5 ± 5% (11.4 ± 14%)
	40–60	1.52 ± 3% (1.44 ± 4%)	43.0 ± 6% (46.5 ± 11%)	28.8 ± 7% (30.2 ± 12%)	14.3 ± 6% (16.3 ± 10%)	13.4 ± 8% (15.7 ± 11%)	510.4 ± 30% (411.8 ± 24%)	88.6 ± 1% (88.8 ± 2%)	1.3 ± 39% (1.4 ± 67%)	10.1 ± 10% (9.8 ± 6%)

BD = Bulk Density, TP = Total Porosity, MaP = Macroporosity, MiP = Microporosity, FC = Field Capacity.

Results are expressed in terms of average and relative standard deviation. The results between parentheses are exclusively for the gallery forest areas, and the results without parentheses are related to the Predominant Land Use (PLU) areas of each micro-catchment.

https://doi.org/10.1371/journal.pone.0179414.t003

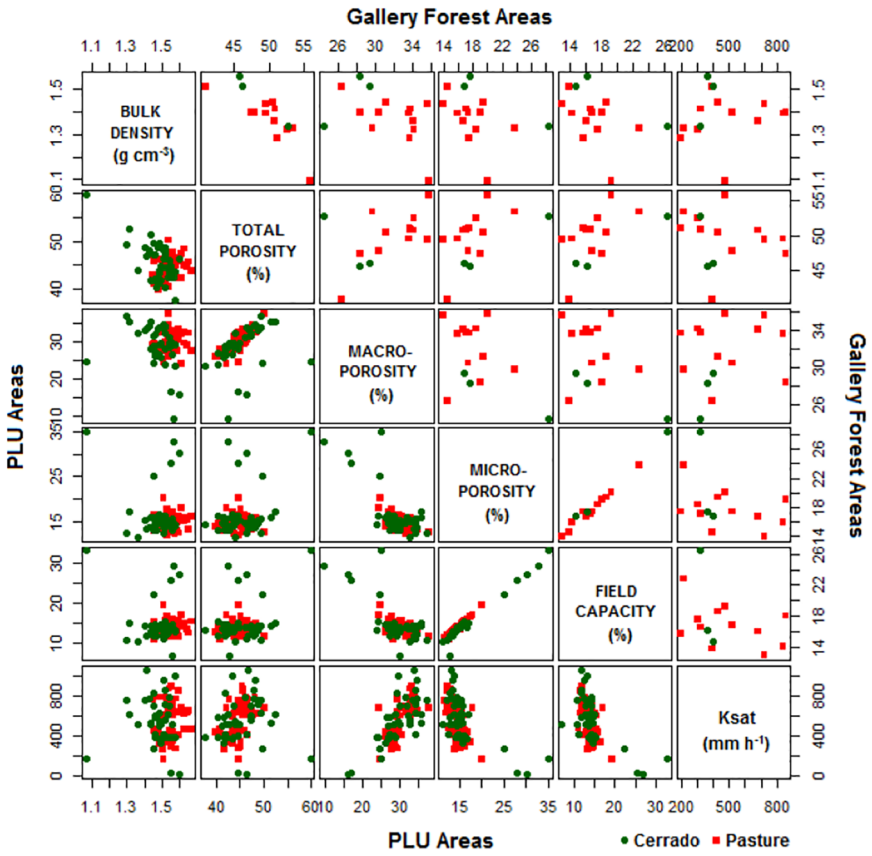

Fig 3. Scatter-plot matrix of soil properties values in the gallery forest (upper panel) and PLU (lower panel) areas in the cerrado and pasture catchments.

https://doi.org/10.1371/journal.pone.0179414.g003

(0.98, $p < .0001$) between the microporosity and the field capacity. The microporosity and macroporosity in both catchments exhibited comparable values, with a predominance of the macroporosity between 60 and 70% of the total porosity. In the PLU areas of the cerrado and pasture catchments, there is a positive correlation between the macroporosity and K_{sat} of 0.74 ($p < .0001$) and 0.68 ($p < .0001$), respectively.

The K_{sat} distribution for the catchments is shown in Fig 4. The K_{sat} values found in the 0–10 cm soil depth in the PLU areas of the cerrado (559.5 ± 38% mm h^{-1}) and pasture (399 ± 40% mm h^{-1}) catchments are significantly different ($p < .05$). Martínez and Zink [93] and Zimmerman et al. [94] also found significantly smaller infiltration rates in pasturelands when compared to nearby areas covered by natural forests. In relation to the rainfall intensities in these catchments, the K_{sat} indicate a high infiltration capacity in both catchments, which generally exceeds the rainfall intensities. This is related to the sandy soil texture and the high macroporosity, which is typical for Arenosols. Our results are in accordance with findings of Scheffler et al. [95] who analyzed soil hydraulic properties of catchments with sandy-loam soil texture ca. 450 km from our study area and found K_{sat} values up to 1,200 mm h^{-1}.

Rainfall characteristics

The monthly total rainfall in each micro-catchment during the two-year study period is shown in Fig 5. Between October 2012 and September 2014, the total rainfall was 3,392 mm in the

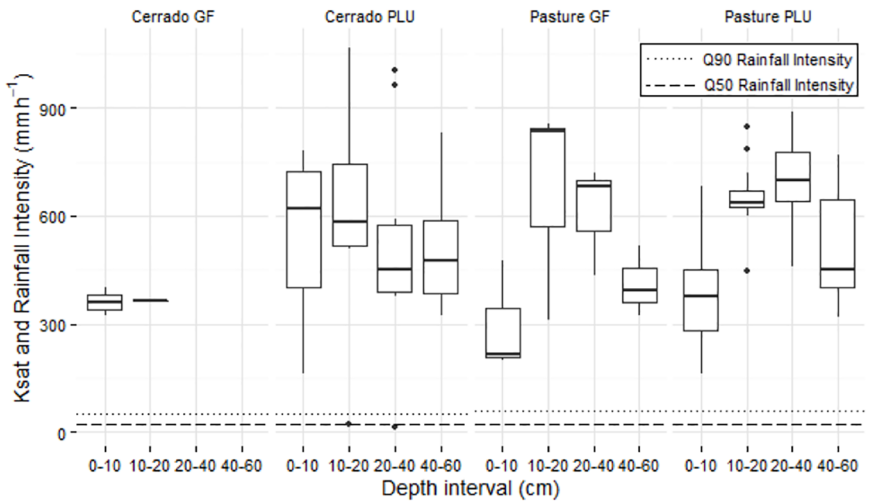

Fig 4. Boxplot of the K_{sat} results, and the 50th and 90th percentiles of the rainfall intensity in the cerrado and pasture catchments.

https://doi.org/10.1371/journal.pone.0179414.g004

cerrado catchment, and 3,560 mm in the pasture catchment. For both catchments, the wet season in 2013–2014 had a smaller contribution to the total annual rainfall than in 2012–2013, which was caused by some atypical rainstorms in the dry season of 2014. The greatest daily rainfall values were recorded on March 2, 2014, for the cerrado catchment, and on January 30, 2013, for the pasture catchment, both at 64 mm d^{-1}.

The difference between the catchments' daily rainfall in the study period is not significant, showing a coefficient of determination of 0.93 ($p < .0001$). We also could not find any significant difference in the rainfall intensity patterns between the cerrado and pasture catchments. In both catchments, the majority of the rainstorms occurred between noon and mid-afternoon with a mean intensity of 28 mm h^{-1}, peaks intensities up to 130 mm h^{-1}, and a duration between 30 and 90 min.

Evapotranspiration

The daily values of E_T are shown in Fig 6. The daily E_T was significantly greater in the cerrado catchment ($p < .0001$). In the PLU areas, the average E_T was 2.7 mm d^{-1} for the cerrado catchment and 1.7 mm d^{-1} for the pasture catchment. In the gallery forest areas, average daily E_T was 3.3 and 2.7 mm d^{-1} for the cerrado and pasture catchments, respectively. The average annual E_T was 1,004 ± 24% mm in the cerrado catchment and 639 ± 31% mm pasture catchment. Our results are comparable to E_T values for cerrado sensu stricto vegetation ranging between 822 and 1,010 mm yr^{-1} found by Giambelluca et al. [32], Oliveira et al. [37], and Dias et al. [96] who applied eddy-covariance measurements, remoting sensing techniques, and a water balance model, respectively. Da Silva et al. [40] found maximum values between 6 and 7 mm d^{-1} during the wet season for an area covered by cerrado vegetation (mostly sensu stricto type), which are in the same range of the maximum values we found.

Our E_T results for the grassland vegetation are in accordance with Dias et al. [96] who used a water balance simulation model and found E_T at 567 mm yr^{-1} in the Cerrado-Amazon ecotone, and with Andrade et al. [36] who used remote sensing techniques and found the daily E_T varying between 1.5 and 2 mm d^{-1} in the Cerrado biome. In a macro-scale analysis for the Mato Grosso state, Lathuillière et al. [33] reported a range of greater values (822–889 mm yr^{-1})

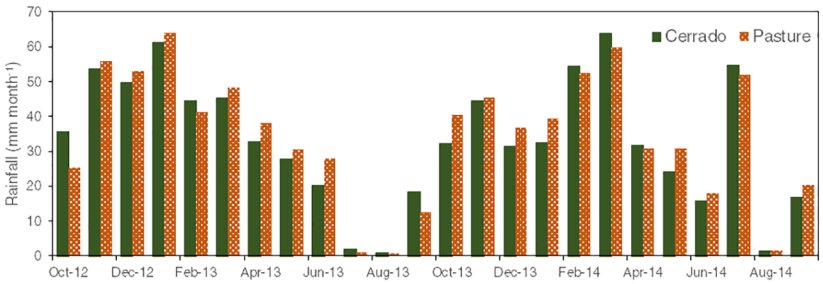

Fig 5. Monthly rainfall per catchment.

https://doi.org/10.1371/journal.pone.0179414.g005

for pasturelands compared to our study; we attribute this difference to the state of degradation of the grassland vegetation in the pasture catchment, which is accredited to reduce the E_T [36].

Streamflow

The daily discharge values are shown in Fig 7. Due to equipment failure, this time series includes some data gaps. The mean stream discharge was 1.24 mm d^{-1} in the cerrado catchment, and 1.96 mm d^{-1} in the pasture catchment. During the wet season, the mean stream discharge was 1.49 mm d^{-1} in the cerrado catchment, and 2.20 mm d^{-1} in the pasture catchment. In the dry season, the stream discharge was 0.92 mm d^{-1} in the cerrado catchment, and 1.58 mm d^{-1} in the pasture catchment.

Table 4 shows a summary of the hydrological indices derived for the study catchments. During the two-year study period, the daily streamflow was significantly greater ($p < .0001$) in the pasture catchment (1,416 ± 7% mm) compared to the cerrado catchment (914 ± 18% mm). We found R_C values of 0.27 for the cerrado and 0.40 for the pasture. Dias et al. (2015) found R_C of 0.25 for a cerrado catchment and 0.58 for a pasture catchment using a model based on water balance equations while Tomasella et al. [97] reported a R_C of 0.38 for a pasture catchment. The flashiness indices are generally small, particularly for the pasture catchment with indices as low as 0.05. The catchment's streamflow decreased by 27% from the wet to the dry season while the decrease in the cerrado catchment was 40%.

The FDCs (Fig 8) of the two catchments show differences in the low flows (Q95) with the cerrado catchment exhibiting the smaller values and greater decrease. Flows with 20% or

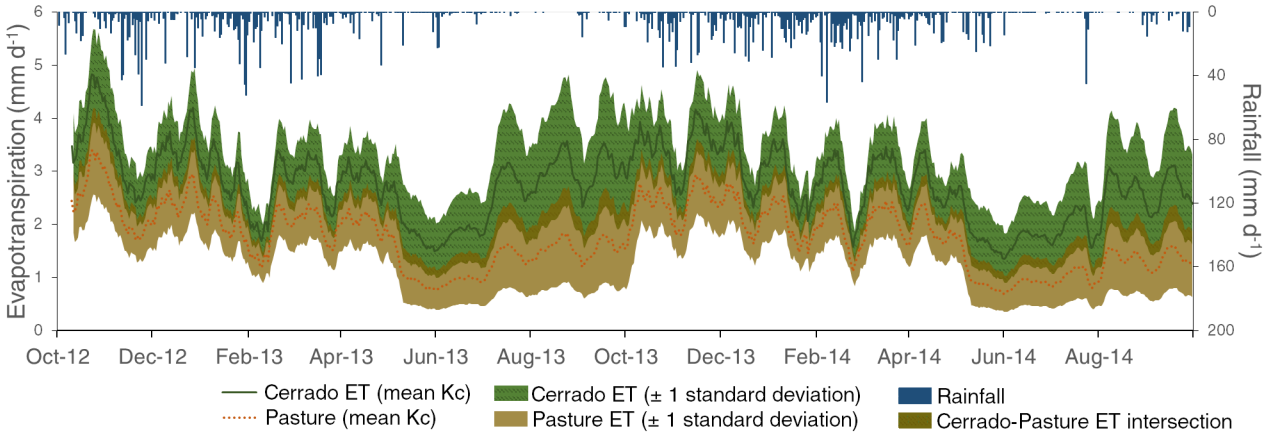

Fig 6. 10-day moving average of evapotranspiration, and daily areal average rainfall for the cerrado and pasture catchments.

https://doi.org/10.1371/journal.pone.0179414.g006

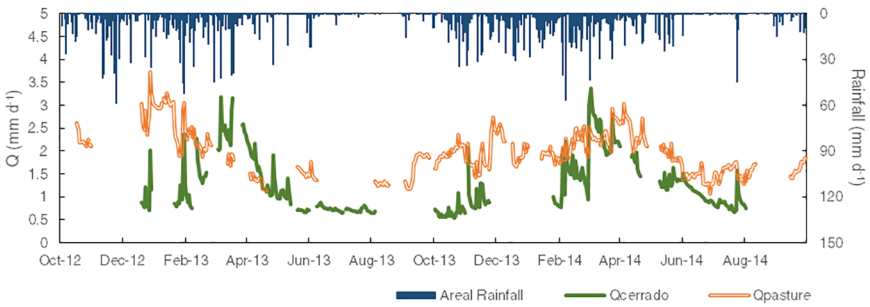

Fig 7. Daily discharges and areal average rainfall for the cerrado and pasture catchments.

https://doi.org/10.1371/journal.pone.0179414.g007

greater probability of exceedance are higher in the pasture than in the cerrado by an average of 82%. The FDCs curves show a flat slope from the middle to the low flows, supporting that low flows are sustained by the baseflow contribution. This is confirmed by the BFI results, which show a high baseflow contribution to total streamflow in both catchments, with ratios higher than 95%. Total quickflow contribution under 5% was also found in other areas of Cerrado at plot [24] and micro-catchment scales [98–100].

Discussion

The pasture catchment showed significantly greater bulk densities and smaller K_{sat} and total porosity at the topsoil. Findings like these have been attributed to soil compaction as a consequence of deforestation, cattle grazing and machinery use, e.g. [101–104]. Although we found significantly smaller K_{sat} values in the pasture catchment, these values exceed the observed peak rainfall intensities, which are likely to restrain Hortonian overflow generation and consequently limit the quickflow contribution (< 5%) to the streamflow in both catchments. Zimmerman et al. [94] found similar results in a study on deforested areas in the Amazon basin, showing that the K_{sat} reduction due to land-use change had no significant impact on quickflow generation in those areas. We associate the K_{sat} results to the high macroporosity in both catchments, which has a known effect on soil permeability [105,106]. While macroporosity values around 10% maintain adequate soil permeability [107], our results show a macroporosity of approximately 30% for both catchments. The presence of macroporosity is related to preferential flow [108], which often limits the overflow generation. In fact, our hydrograph analysis shows that baseflow is a major driver of streamflow in both catchments, with BFI over 95%.

Table 5 shows a compilation of the daily and annual E_T and Q results for both catchments. The cerrado catchment had the greater E_T compared with the pasture catchment. While the mean E_T decreased 45% in the pasture catchment from the wet to the dry season, the E_T in the cerrado catchment was reduced by 24%. We attribute this result to the canopy cover in the

Table 4. Total streamflow and hydrological indices.

	Cerrado		Pasture	
	2012–2013	2013–2014	2012–2013	2013–2014
Mean streamflow (mm yr^{-1})	453	461	724	692
Runoff Coefficient (R_C)	0.29	0.25	0.45	0.35
Flashiness	0.1145	0.1015	0.0567	0.0517
Baseflow Index (BFI)	0.96	0.97	0.98	0.96

https://doi.org/10.1371/journal.pone.0179414.t004

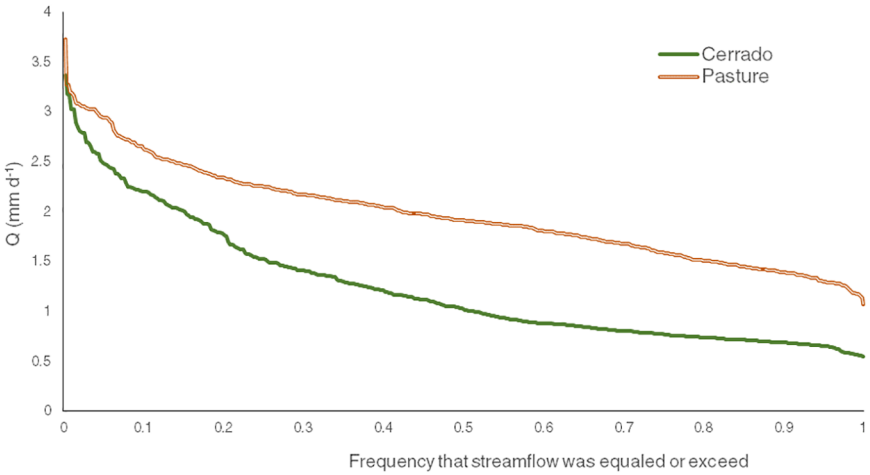

Fig 8. Flow-duration curves of daily discharge for the cerrado and pasture catchments.

https://doi.org/10.1371/journal.pone.0179414.g008

Table 5. Daily and annual evapotranspiration and streamflow rates.

Catchment	Evapotranspiration			Streamflow		
	Dry (mm d^{-1})	Wet (mm d^{-1})	Annual (mm yr^{-1})	Dry (mm d^{-1})	Wet (mm d^{-1})	Annual (mm yr^{-1})
Cerrado	2.32 ± 24%	3.06 ± 26%	1,004 ± 24%	0.92 ± 27%	1.49 ± 46%	457 ± 18%
Pasture	1.19 ± 44%	2.15 ± 27%	639 ± 31%	1.58 ± 15%	2.20 ± 20%	708 ± 7%

https://doi.org/10.1371/journal.pone.0179414.t005

cerrado vegetation with leaf area index values ranging from approximately 0.7 to 1.1 throughout the year [109] and with root lengths sufficient to reach deep soil horizons [56], which ensures E_T rates at 2.32 ± 24% mm d^{-1} during the dry season.

E_T is a major component of the water balance in tropical regions [5]. As reported in other studies [50,110], the differences in E_T between native vegetation and grassland plays a major role in the streamflow dynamics. Our results confirms trend analyses and water balance modelling studies at the macro-scale (*das Mortes* River basin), which show an increase of streamflow due to the deforestation of the cerrado vegetation [29,111]. In fact, the conversion of native vegetation to croplands and pasturelands in the Mato Grosso state resulted in a 25% decrease in E_T [33], and that water export increases up to fourfold in agricultural areas due to the reduction of E_T [112]. Our results are also consistent with those of other studies that reported decreases in E_T [37,96] and increases in discharge [26,28,42,47,113–116] due to conversion of natural vegetation to grasslands on the Amazonian agricultural frontier.

Results from other tropical catchments studies that show a decrease in dry season streamflow as a consequence of forest conversion [51,117] cannot be confirmed in our study in the Cerrado biome. From the wet to the dry season our results showed a greater decrease in streamflow in the cerrado catchment than in the pasture catchment, while the E_T behaved otherwise with lower decrease in the cerrado catchment. We suggest that this is related to the higher root zone storage capacity of the cerrado vegetation. The deep roots of the cerrado vegetation influence the water balance and appear to be important in proving water for vegetation during the dry season [118]. Indeed, the cerrado vegetation is highly adapted to a long dry season and deeply weathered soils [27], which is a particular situation that demands more detailed hydrological research in this region. The replacement of the cerrado vegetation with exotic

grasses seems to increase the deep seepage and reduce E_T, which in turn will increase the streamflow, especially during the dry season.

Conclusions

We investigated the hydrological responses of two headwater micro-catchments with contrasting land use (cerrado vs. pasture) in the Brazilian Cerrado using field data collected between 2012 and 2014. From our study, we conclude that the conversion of the undisturbed cerrado to pasture caused:

1. Significant soil hydro-physical degradation as indicated by higher bulk density and reduced soil porosity in the pasture catchment in comparison to the cerrado catchment;
2. An increase in streamflow as shown by the significantly greater daily and annual streamflow values in the pasture catchment. Furthermore, we conclude that cerrado conversion to pasture reduced the evapotranspiration.

While our study contributes to understanding of the soil degradation and hydrological processes in this region, we suggest long-term measurements including quantifying changes in groundwater storage in order to better clarify the mechanisms causing the observed behavior in our data.

Acknowledgments

This research was feasible thanks to the collaboration of field site hosts (*Fazenda Gianetta* and *Fazenda Rancho do Sol*). The authors also acknowledge: Jonas Macedo, Norma Bertão and Túlio Santos for the field assistance; Prof. J. Cunha for the advises concerning the SEBAL and METRIC application; and Dr. J. Grotheer for technical support. We also thank the anonymous reviewers for the helpful comments.

Author Contributions

Conceptualization: RLBN ACG GG RSSA.

Data curation: RLBN ACG GNT KK GL RSSA.

Formal analysis: RLBN ACG KK GNT RSSA.

Funding acquisition: GG RSSA EC.

Investigation: RLBN ACG GNT GL.

Methodology: RLBN ACG RSSA GG.

Project administration: RLBN ACG RSSA GG EC.

Resources: GG RSSA EC.

Software: RLBN.

Supervision: ACG RSSA GG EC.

Validation: RLBN ACG GL GG.

Visualization: RLBN KK.

Writing – original draft: RLBN ACG GL GG.

Writing – review & editing: RLBN ACG GNT KK GL RSSA EC GG.

References

1. Sanchez-Azofeifa GA, Quesada M, Rodriguez JP, Nassar JM, Stoner KE, Castillo A, et al. Research Priorities for Neotropical Dry Forests1. Biotropica. 2005; 37: 477–485. https://doi.org/10.1111/j.1744-7429.2005.00066.x
2. Santos JC, Leal IR, Almeida-Cortez JS, Fernandes GW, Tabarelli M. Caatinga: the scientific negligence experienced by a dry tropical forest. Trop Conserv Sci. 2011; 4: 276–286. Available: http://tropicalconservationscience.mongabay.com/content/v4/11-09-25_276-286_Santos_et_al.pdf
3. Farrick KK, Branfireun BA. Left high and dry: a call to action for increased hydrological research in tropical dry forests. Hydrol Process. 2013; 3262: 3254–3262. https://doi.org/10.1002/hyp.9935
4. Miles L, Newton AC, DeFries RS, Ravilious C, May I, Blyth S, et al. A global overview of the conservation status of tropical dry forests. J Biogeogr. 2006; 33: 491–505. https://doi.org/10.1111/j.1365-2699.2005.01424.x
5. Wohl E, Barros A, Brunsell N, Chappell NA, Coe M, Giambelluca T, et al. The hydrology of the humid tropics. Nat Clim Chang. Nature Publishing Group; 2012; 2: 655–662. https://doi.org/10.1038/nclimate1556
6. Smith J, Winograd M, Gallopin G, Pachico D. Dynamics of the agricultural frontier in the Amazon and savannas of Brazil: analyzing the impact of policy and technology. Environ Model Assess. 1998; 3: 31–46. https://doi.org/10.1023/A:1019094218552
7. Klink CA, Machado RB. Conservation of the Brazilian Cerrado. Conserv Biol. 2005; 19: 707–713. https://doi.org/10.1111/j.1523-1739.2005.00702.x
8. Sano EE, Rosa R, Brito JLS, Ferreira LG. Mapeamento semidetalhado do uso da terra do Bioma Cerrado. Pesqui Agropecuária Bras. 2008; 43: 153–156. https://doi.org/10.1590/S0100-204X2008000100020
9. Beuchle R, Grecchi RC, Shimabukuro YE, Seliger R, Eva HD, Sano E, et al. Land cover changes in the Brazilian Cerrado and Caatinga biomes from 1990 to 2010 based on a systematic remote sensing sampling approach. Appl Geogr. 2015; 58: 116–127. https://doi.org/10.1016/j.apgeog.2015.01.017
10. Myers N, Mittermeier RA, Mittermeier CG, da Fonseca GAB, Kent J. Biodiversity hotspots for conservation priorites. Nature. 2000; 403: 853–858. https://doi.org/10.1038/35002501 PMID: 10706275
11. Lapola DM, Schaldach R, Alcamo J, Bondeau A, Msangi S, Priess JA, et al. Impacts of Climate Change and the End of Deforestation on Land Use in the Brazilian Legal Amazon. Earth Interact. 2011; 15: 1–29. https://doi.org/10.1175/2010EI333.1
12. Lapola DM, Martinelli LA, Peres CA, Ometto JPHB, Ferreira ME, Nobre CA, et al. Pervasive transition of the Brazilian land-use system. Nat Clim Chang. 2013; 4: 27–35. https://doi.org/10.1038/nclimate2056
13. Brown AE, Zhang L, McMahon TA, Western AW, Vertessy RA. A review of paired catchment studies for determining changes in water yield resulting from alterations in vegetation. J Hydrol. 2005; 310: 28–61. https://doi.org/10.1016/j.jhydrol.2004.12.010
14. Neill C, Coe MT, Riskin SH, Krusche A V., Elsenbeer H, Macedo MN, et al. Watershed responses to Amazon soya bean cropland expansion and intensification. Philos Trans R Soc B Biol Sci. 2013; 368: 20120425–20120425. https://doi.org/10.1098/rstb.2012.0425 PMID: 23610178
15. Recha JW, Lehmann J, Walter MT, Pell A, Verchot L, Johnson M. Stream Discharge in Tropical Headwater Catchments as a Result of Forest Clearing and Soil Degradation. Earth Interact. 2012; 16: 1–18. https://doi.org/10.1175/2012EI000439.1
16. Williams MR, Melack JM. Solute export from forested and partially deforested catchments in the central Amazon. Biogeochemistry. 1997; 38: 67–102. https://doi.org/10.1023/A:1005774431820
17. Neill C, Deegan LA, Thomas SM, Cerri CC. Deforestation for pasture alters nitrogen and phosphorus in small Amazonian streams. Ecol Appl. 2001; 11: 1817–1828. https://doi.org/10.1890/1051-0761(2001)011[1817:DFPANA]2.0.CO;2
18. Ballester M. A remote sensing/GIS-based physical template to understand the biogeochemistry of the Ji-Paraná river basin (Western Amazônia). Remote Sens Environ. 2003; 87: 429–445. https://doi.org/10.1016/j.rse.2002.10.001
19. Germer S, Neill C, Vetter T, Chaves J, Krusche A V., Elsenbeer H. Implications of long-term land-use change for the hydrology and solute budgets of small catchments in Amazonia. J Hydrol. 2009; 364: 349–363. https://doi.org/10.1016/j.jhydrol.2008.11.013
20. Figueiredo RO, Markewitz D, Davidson EA, Schuler AE, dos S. Watrin O, de Souza Silva P. Land-use effects on the chemical attributes of low-order streams in the eastern Amazon. J Geophys Res. 2010; 115: G04004. https://doi.org/10.1029/2009JG001200

21. Richey JE, Ballester MV, Davidson EA, Johnson MS, Krusche A V. Land-Water interactions in the amazon. Biogeochemistry. 2011; 105: 1–5. https://doi.org/10.1007/s10533-011-9622-y

22. Jepson W, Brannstrom C, Filippi A. Access Regimes and Regional Land Change in the Brazilian Cerrado, 1972–2002. Ann Assoc Am Geogr. Routledge; 2010; 100: 87–111. https://doi.org/10.1080/00045600903378960

23. Hunke P, Roller R, Zeilhofer P, Schröder B, Mueller EN, Nora E. Soil changes under different land-uses in the Cerrado of Mato Grosso, Brazil. Geoderma Reg. Elsevier B.V.; 2015; 4: 31–43. https://doi.org/10.1016/j.geodrs.2014.12.001

24. Oliveira PTS, Wendland E, Nearing M a., Scott RL, Rosolem R, da Rocha HR. The water balance components of undisturbed tropical woodlands in the Brazilian cerrado. Hydrol Earth Syst Sci. 2015; 19: 2899–2910. https://doi.org/10.5194/hess-19-2899-2015

25. Alho CJR. Importância da biodiversidade para a saúde humana: uma perspectiva ecológica. Estud Avançados. 2012; 26: 151–166. https://doi.org/10.1590/S0103-40142012000100011

26. Davidson EA, de Araújo AC, Artaxo P, Balch JK, Brown IF, C. Bustamante MM, et al. The Amazon basin in transition. Nature. 2012; 481: 321–328. https://doi.org/10.1038/nature10717 PMID: 22258611

27. Hunke P, Mueller EN, Schröder B, Zeilhofer P. The Brazilian Cerrado: assessment of water and soil degradation in catchments under intensive agricultural use. Ecohydrology. 2015; 8: 1154–1180. https://doi.org/10.1002/eco.1573

28. Costa MH, Botta A, Cardille JA. Effects of large-scale changes in land cover on the discharge of the Tocantins River, Southeastern Amazonia. J Hydrol. 2003; 283: 206–217. https://doi.org/10.1016/S0022-1694(03)00267-1

29. Guzha AC, Nóbrega R, Kovacs K, Amorim RSS, Gerold G. Quantifying impacts of agro-industrial expansion in Mato Grosso, Brazil, on watershed hydrology using the Soil and Water Assessment Tool (SWAT) model. Proceedings of the 20th International Congress on Modelling and Simulation, Adelaide, Australia, 1–6 December. 2013. pp. 1833–1839.

30. Juhász CEP, Cooper M, Cursi PR, Ketzer AO, Toma RS. Savanna woodland soil micromorphology related to water retention. Sci Agric. 2007; 64: 344–354. https://doi.org/10.1590/S0103-90162007000400005

31. da Rocha HR, Manzi AO, Cabral OM, Miller SD, Goulden ML, Saleska SR, et al. Patterns of water and heat flux across a biome gradient from tropical forest to savanna in Brazil. J Geophys Res. 2009; 114: G00B12. https://doi.org/10.1029/2007JG000640

32. Giambelluca TW, Scholz FG, Bucci SJ, Meinzer FC, Goldstein G, Hoffmann WA, et al. Evapotranspiration and energy balance of Brazilian savannas with contrasting tree density. Agric For Meteorol. 2009; 149: 1365–1376. https://doi.org/10.1016/j.agrformet.2009.03.006

33. Lathuillière MJ, Johnson MS, Donner SD. Water use by terrestrial ecosystems: temporal variability in rainforest and agricultural contributions to evapotranspiration in Mato Grosso, Brazil. Environ Res Lett. 2012; 7: 24024. https://doi.org/10.1088/1748-9326/7/2/024024

34. Scherer-Warren M. Desmembramento de Estimativas de Evapotranspiração Obtidas por Sensoriamento Remoto nas Componentes de Evaporação e Transpiração Vegetal. Rev Bras Geogr Física. 2012; 361–373.

35. Scherer-Warren M, Rodrigues LN. Estimativa de Evapotranspiração Real por Sensoriamento Remoto: procedimento e aplicação em pivô central. Planaltina; 2013.

36. Andrade RG, de C. Teixeira AH, Sano EE, Leivas JF, de C. Victoria D, Nogueira SF. Pasture evapotranspiration as indicators of degradation in the Brazilian Savanna: a case study for Alto Tocantins watershed. 2014; 9239: 92391Z. https://doi.org/10.1117/12.2067225

37. Oliveira PTS, Nearing MA, Moran MS, Goodrich DC, Wendland E, Gupta H V. Trends in water balance components across the Brazilian Cerrado. Water Resour Res. 2014; 50: 7100–7114. https://doi.org/10.1002/2013WR015202

38. Ataíde KRP, Baptista GM de M. Modelagem de determinação da evapotranspiração real para o bioma. Proceedings of XVII Simpósio Brasileiro de Sensoriamento Remoto—SBSR, João Pessoa-PB, Brazil, INPE. 2015. pp. 6381–6388.

39. Sano EE, Ferreira LG, Asner GP, Steinke ET. Spatial and temporal probabilities of obtaining cloud-free Landsat images over the Brazilian tropical savanna. Int J Remote Sens. 2007; 28: 2739–2752. https://doi.org/10.1080/01431160600981517

40. da Silva BB, Wilcox BP, da Silva V de PR, Montenegro SMGL, de Oliveira LMM. Changes to the energy budget and evapotranspiration following conversion of tropical savannas to agricultural lands in São Paulo State, Brazil. Ecohydrology. 2015; 8: 1272–1283. https://doi.org/10.1002/eco.1580

41. Burt TP, McDonnell JJ. Whither field hydrology? The need for discovery science and outrageous hydrological hypotheses. Water Resour Res. 2015; 51: 5919–5928. https://doi.org/10.1002/2014WR016839

42. Guzha AC, Nobrega RLB, Kovacs K, Rebola-Lichtenberg J, Amorim RSS, Gerold G. Characterizing rainfall-runoff signatures from micro-catchments with contrasting land cover characteristics in southern Amazonia. Hydrol Process. 2015; 29: 508–521. https://doi.org/10.1002/hyp.10161

43. Jepson W. A disappearing biome? Reconsidering land-cover change in the Brazilian savanna. Geogr J. 2005; 171: 99–111. https://doi.org/10.1111/j.1475-4959.2005.00153.x

44. Schneider R. Ground-Water Provinces of Brazil. Washington; 1963.

45. Ratter J, Ribeiro JF, Bridgewater S. The Brazilian Cerrado Vegetation and Threats to its Biodiversity. Ann Bot. 1997; 80: 223–230. https://doi.org/10.1006/anbo.1997.0469

46. Marcuzzo FFN, Melo DCR, Rocha HM. Distribuição Espaço-Temporal e Sazonalidade das Chuvas no Estado do Mato Grosso. Rev Bras Recur Hídricos. 2011; 16: 157–167.

47. de Moraes JM, Schuler AE, Dunne T, Figueiredo R de O, Victoria RL. Water storage and runoff processes in plinthic soils under forest and pasture in eastern Amazonia. Hydrol Process. 2006; 20: 2509–2526. https://doi.org/10.1002/hyp.6213

48. Germer S, Neill C, Krusche A V., Elsenbeer H. Influence of land-use change on near-surface hydrological processes: Undisturbed forest to pasture. J Hydrol. 2010; 380: 473–480. https://doi.org/10.1016/j.jhydrol.2009.11.022

49. Roa-García MC, Brown S, Schreier H, Lavkulich LM. The role of land use and soils in regulating water flow in small headwater catchments of the Andes. Water Resour Res. 2011; 47: W05510. https://doi.org/10.1029/2010WR009582

50. Muñoz-Villers LE, McDonnell JJ. Land use change effects on runoff generation in a humid tropical montane cloud forest region. Hydrol Earth Syst Sci. 2013; 17: 3543–3560. https://doi.org/10.5194/hess-17-3543-2013

51. Ogden FL, Crouch TD, Stallard RF, Hall JS. Effect of land cover and use on dry season river runoff, runoff efficiency, and peak storm runoff in the seasonal tropics of Central Panama. Water Resour Res. 2013; 49: 8443–8462. https://doi.org/10.1002/2013WR013956

52. Troch PA, Lahmers T, Meira A, Mukherjee R, Pedersen JW, Roy T, et al. Catchment coevolution: A useful framework for improving predictions of hydrological change? Water Resour Res. 2015; 51: 4903–4922. https://doi.org/10.1002/2015WR017032

53. Goodland R. A physiognomic analysis of the Cerrado vegetation of Central Brasil. J Ecol. 1971; 59: 411–419. https://doi.org/10.2307/2258321

54. Goodland R, Pollard R. The Brazilian Cerrado Vegetation: A Fertility Gradient. J Ecol. 1973; 61: 219–224. https://doi.org/10.2307/2258929

55. Furley PA. The nature and diversity of neotropical savanna vegetation with particular reference to the Brazilian cerrados. Glob Ecol Biogeogr. 1999; 8: 223–241. https://doi.org/10.1046/j.1466-822X.1999.00142.x

56. Canadell J, Jackson RB, Ehleringer JB, Mooney H a., Sala OE, Schulze E-D. Maximum rooting depth of vegetation types at the global scale. Oecologia. 1996; 108: 583–595. https://doi.org/10.1007/BF00329030 PMID: 28307789

57. IUSS Working Group WRB. World Reference Base for Soil Resources 2014, update 2015. International soil classification system for naming soils and creating legends for soil maps. World Soil Resources Reports No. 106. Rome; 2015.

58. Soil Survey Staff. Illustrated guide to soil taxonomy. Igarss 2014. Lincoln, Nebraska; 2014.

59. EMBRAPA. Sistema brasileiro de classificação de solos. 2nd ed. Rio de Janeiro: EMBRAPA-SPI; 2006.

60. Marimon BS, Felfili JM, Lima EDS, Duarte WMG, Marimon-Júnior BH. Environmental determinants for natural regeneration of gallery forest at the Cerrado/Amazonia boundaries in Brazil. Acta Amaz. 2010; 40: 107–118. https://doi.org/10.1590/S0044-59672010000100014

61. Felfili JM., Silva Júnior MC. Floristic composition, phytosociology and comparison of cerrado and gallery forests at Fazenda Água Limpa, Federal District, Brazil. In: Furley P. A.; Proctor J.; Ratter JA, editor. Nature and Dynamics of Forest-Savanna Boundaries. London: Chapman and Hall; 1992. pp. 393–415.

62. Felfili JM, Mendonça RC, Walter BMT, Silva Júnior MC, Nóbrega MGG, Fagg CW, et al. Flora fanerogâmica das matas de galeria e ciliares do Brasil Central. In: Ribeiro, J. F.; Fonseca, C. E. L.; Silva; Souza-Silva JC, editor. Cerrado: caracterização e recuperação de Matas de Galeria. Planaltina, Brazil: EMBRAPA/Cerrados; 2001. pp. 195–263.

63. Moore ID, Grayson RB, Ladson AR. Digital terrain modelling: A review of hydrological, geomorphological, and biological applications. Hydrol Process. 1991; 5: 3–30. https://doi.org/10.1002/hyp.3360050103

64. Gessler PE, Moore ID, McKenzie NJ, Ryan PJ. Soil-landscape modelling and spatial prediction of soil attributes. Int J Geogr Inf Syst. 1995; 9: 421–432. https://doi.org/10.1080/02693799508902047

65. Evans JS. An ArcGIS Toolbox for surface gradient and geomorphometric modeling, version 2.0–0 [Internet]. 2014 [cited 15 May 2015]. Available: http://evansmurphy.wix.com/evansspatial

66. Voltz M, Goulard M. Spatial interpolation of soil moisture retention curves. Geoderma. 1994; 62: 109–123. https://doi.org/10.1016/0016-7061(94)90031-0

67. Chaplot V, Walter C, Curmi P, Hollier-Larousse A. The use of auxiliary geophysical data to improve a soil-landscape model. Soil Sci. 2000; 165: 961–970. https://doi.org/10.1097/00010694-200012000-00006

68. Montanari R, Souza GSA, Pereira GT, Marques J, Siqueira DS, Siqueira GM. The use of scaled semivariograms to plan soil sampling in sugarcane fields. Precis Agric. 2012; 13: 542–552. https://doi.org/10.1007/s11119-012-9265-6

69. Herbst M, Diekkrüger B. The influence of the spatial structure of soil properties on water balance modeling in a microscale catchment. Phys Chem Earth, Parts A/B/C. 2002; 27: 701–710. https://doi.org/10.1016/S1474-7065(02)00054-2

70. Herbst M, Diekkrüger B, Vereecken H. Geostatistical co-regionalization of soil hydraulic properties in a micro-scale catchment using terrain attributes. Geoderma. 2006; 132: 206–221. https://doi.org/10.1016/j.geoderma.2005.05.008

71. Gee GW. Particle-size analysis. In: Klute A, editor. Methods of soil analysis. 2nd ed. Madison, WI: ASA and SSSA; 1986. pp. 383–411.

72. Burke W, Gabriels D, Bouma J. Soil structure assessment. Rotterdam: Balkema Publishers; 1986.

73. EMBRAPA. Manual de Métodos de Análise de Solo. 2nd ed. Rio de Janeiro: EMBRAPA-CNPS; 1997.

74. Richards LA. Pressure-membrane apparatus, construction and use. Agriculrural Eng. 1947; 451–454.

75. ASCE-EWRI. The ASCE standardized reference evapotranspiration equation. ASCE-EWRI Standardization of Reference Evapotranspiration Task Comm. Report. ASCE Bookstore; 2005.

76. Allen R, Irmak A, Trezza R, Hendrickx JMH, Bastiaanssen W, Kjaersgaard J. Satellite-based ET estimation in agriculture using SEBAL and METRIC. Hydrol Process. 2011; 25: 4011–4027. https://doi.org/10.1002/hyp.8408

77. Bastiaanssen WGM, Menenti M, Feddes RA, Holtslag AAM. A remote sensing surface energy balance algorithm for land (SEBAL). 1. Formulation. J Hydrol. 1998; 212–213: 198–212. https://doi.org/10.1016/S0022-1694(98)00253-4

78. Bastiaanssen WG. SEBAL-based sensible and latent heat fluxes in the irrigated Gediz Basin, Turkey. J Hydrol. 2000; 229: 87–100. https://doi.org/10.1016/S0022-1694(99)00202-4

79. Allen RG, Tasumi M, Trezza R, Morse A, Trezza R, Wright JL, et al. Satellite-Based Energy Balance for Mapping Evapotranspiration with Internalized Calibration (METRIC)—Model. J Irrig Drain Eng. 2007; 133: 380–394. https://doi.org/10.1061/(ASCE)0733-9437(2007)133:4(380)

80. Ruhoff AL, Paz AR, Collischonn W, Aragao LEOC, Rocha HR, Malhi YS. A MODIS-Based Energy Balance to Estimate Evapotranspiration for Clear-Sky Days in Brazilian Tropical Savannas. Remote Sens. 2012; 4: 703–725. https://doi.org/10.3390/rs4030703

81. Paço TA, Pôças I, Cunha M, Silvestre JC, Santos FL, Paredes P, et al. Evapotranspiration and crop coefficients for a super intensive olive orchard. An application of SIMDualKc and METRIC models using ground and satellite observations. J Hydrol. Elsevier B.V.; 2014; 519: 2067–2080. https://doi.org/10.1016/j.jhydrol.2014.09.075

82. Mkhwanazi M, Chávez J, Andales A. SEBAL-A: A Remote Sensing ET Algorithm that Accounts for Advection with Limited Data. Part I: Development and Validation. Remote Sens. 2015; 7: 15046–15067. https://doi.org/10.3390/rs71115046

83. Jarvis A, Reuter HI, Nelson A, Guevara E. Hole-filled seamless SRTM data V4, International Centre for Tropical Agriculture (CIAT) [Internet]. Dec 2008 [cited 1 Jan 2015]. Available: http://srtm.csi.cgiar.org

84. Chander G, Markham BL, Helder DL. Summary of current radiometric calibration coefficients for Landsat MSS, TM, ETM+, and EO-1 ALI sensors. Remote Sens Environ. Elsevier Inc.; 2009; 113: 893–903. https://doi.org/10.1016/j.rse.2009.01.007

85. Allen RG, Pereira LS, Raes D, Smith M. Crop evapotranspiration: Guidelines for computing crop requirements. Irrig Drain Pap No 56, FAO. 1998; 300. 10.1016/j.eja.2010.12.001

86. USGS. Preliminary Assessment of Landsat 7 ETM+ Data Following Scan Line Corrector Malfunction [Internet]. 2003. Available: http://landsat.usgs.gov/documents/SLC_off_Scientific_Usability.pdf

87. Eckhardt K. How to construct recursive digital filters for baseflow separation. Hydrol Process. 2005; 19: 507–515. https://doi.org/10.1002/hyp.5675

88. Lim KJ, Engel BA, Tang Z, Choi J, Kim K-S, Muthukrishnan S, et al. Automated Web GIS based hydrograph analysis tool, WHAT. J Am Water Resour Assoc. 2005; 41: 1407–1416. https://doi.org/10.1111/j.1752-1688.2005.tb03808.x

89. Lim KJ, Park YS, Kim J, Shin Y-C, Kim NW, Kim SJ, et al. Development of genetic algorithm-based optimization module in WHAT system for hydrograph analysis and model application. Comput Geosci. 2010; 36: 936–944. https://doi.org/10.1016/j.cageo.2010.01.004

90. Vogel RM, Fennessey NM. Flow-Duration Curves. I: New Interpretation and Confidence Intervals. J Water Resour Plan Manag. 1994; 120: 485–504. https://doi.org/10.1061/(ASCE)0733-9496(1994)120:4(485)

91. Baker DB, Richards RP, Loftus TT, Kramer JW. A new flashiness index: characteristics and applications to midwestern rivers and streams. J Am Water Resour Assoc. 2004; 40: 503–522. https://doi.org/10.1111/j.1752-1688.2004.tb01046.x

92. Valpassos MAR, Cavalcante EGS, Cassiolato AMR, Alves MC. Effects of soil management systems on soil microbial activity, bulk density and chemical properties. Pesqui Agropecuária Bras. 2001; 36: 1539–1545. https://doi.org/10.1590/S0100-204X2001001200011

93. Martínez LJ, Zinck JA. Temporal variation of soil compaction and deterioration of soil quality in pasture areas of Colombian Amazonia. Soil Tillage Res. 2004; 75: 3–18. https://doi.org/10.1016/j.still.2002.12.001

94. Zimmermann B, Elsenbeer H, De Moraes JM. The influence of land-use changes on soil hydraulic properties: Implications for runoff generation. For Ecol Manage. 2006; 222: 29–38. https://doi.org/10.1016/j.foreco.2005.10.070

95. Scheffler R, Neill C, Krusche A V., Elsenbeer H. Soil hydraulic response to land-use change associated with the recent soybean expansion at the Amazon agricultural frontier. Agric Ecosyst Environ. Elsevier B.V.; 2011; 144: 281–289. https://doi.org/10.1016/j.agee.2011.08.016

96. Dias LCP, Macedo MN, Costa MH, Coe MT, Neill C. Effects of land cover change on evapotranspiration and streamflow of small catchments in the Upper Xingu River Basin, Central Brazil. J Hydrol Reg Stud. Elsevier B.V.; 2015; 4: 108–122. https://doi.org/10.1016/j.ejrh.2015.05.010

97. Tomasella J, Neill C, Figueiredo R, Nobre AD. Water and chemical budgets at the catchment scale including nutrient exports from intact forests and disturbed landscapes. Geophysical Monograph Series. 2009. pp. 505–524. https://doi.org/10.1029/2008GM000727

98. Lima JEFW. Determinação da evapotranspiração de uma bacia hidrográfica sob vegetação natural de cerrado, pelo método do balanço hídrico. Universidade de Brasília, Brasília, Brazil. 2000.

99. Silva CL, Oliveira CAS. Runoff measurement and prediction for a watershed under natural vegetation in central Brazil. Rev Bras Ciência do Solo. 1999; 23: 695–701. https://doi.org/10.1590/S0100-06831999000300024

100. Alencar DBS de, Silva CL da, Oliveira CA da S. Influência da precipitação no escoamento superficial em uma microbacia hidrográfica do Distrito Federal. Eng Agrícola. 2006; 26: 103–112. https://doi.org/10.1590/S0100-69162006000100012

101. De Oliveira OC, De Oliveira IP, Alves BJR, Urquiaga S, Boddey RM. Chemical and biological indicators of decline/degradation of Brachiaria pastures in the Brazilian Cerrado. Agric Ecosyst Environ. 2004; 103: 289–300. https://doi.org/10.1016/j.agee.2003.12.004

102. Hamza MA, Anderson WK. Soil compaction in cropping systems: A review of the nature, causes and possible solutions. Soil and Tillage Research. 2005. pp. 121–145. https://doi.org/10.1016/j.still.2004.08.009

103. Drewry JJ, Cameron KC, Buchan GD. Pasture yield and soil physical property responses to soil compaction from treading and grazing—A review. Australian Journal of Soil Research. 2008. pp. 237–256. https://doi.org/10.1071/SR07125

104. Greenwood KL, McKenzie BM. Grazing effects on soil physical properties and the consequences for pastures: a review. Aust J Exp Agric. 2001; 41: 1231–1250.

105. Logsdon SD, Allmaras RR, Wu L, Swan JB, Randall GW. Macroporosity and Its Relation to Saturated Hydraulic Conductivity under Different Tillage Practices. Soil Sci Soc Am J. 1990; 54: 1096. https://doi.org/10.2136/sssaj1990.03615995005400040029x

106. Lin HS, McInnes KJ, Wilding LP, Hallmark CT. Macroporosity and initial moisture effects on infiltration rates in vertisols and vertic intergrades. Soil Sci. 1998; 163: 2–8. https://doi.org/10.1097/00010694-199801000-00002

107. Carter MR. Temporal variability of soil macroporosity in a fine sandy loam under mouldboard ploughing and direct drilling. Soil Tillage Res. 1988; 12: 37–51. https://doi.org/10.1016/0167-1987(88)90054-2

108. Diab M, Merot P, Curmi P. Water Movement in a glossaqualf as measured by two tracers. Geoderma. 1988; 43: 143–161. https://doi.org/10.1016/0016-7061(88)90040-7

109. Hoffmann WA, da Silva ER, Machado GC, Bucci SJ, Scholz FG, Goldstein G, et al. Seasonal leaf dynamics across a tree density gradient in a Brazilian savanna. Oecologia. 2005; 145: 306–315. https://doi.org/10.1007/s00442-005-0129-x PMID: 15965754

110. Bruijnzeel LA. Tropical montane cloud forest: a unique hydrological case. In: Bonell M; Bruijnzeel LA, editor. Forests, Water and People in the Humid Tropics. Cambridge, UK: Cambridge Univ. Press; 2005. pp. 462–483.

111. Guzha AC, Nobrega R, Santos CAG, Gerold G. Investigating discharge and rainfall variability in an Amazonian watershed: Do any trends exist? Proceedings of H01, IAHS-IAPSO-IASPEI Assembly. Gothenburg, Sweden: IAHS; 2013. pp. 346–351.

112. Neill C, Coe MT, Riskin SH, Krusche A V, Elsenbeer H, Marcia N, et al. Watershed responses to Amazon soya bean cropland expansion and intensification Watershed responses to Amazon soya bean cropland expansion and intensification. 2013;

113. Neill C, Chaves JE, Biggs T, Deegan LA, Elsenbeer H, Figueiredo RO, et al. Runoff sources and land cover change in the Amazon: an end-member mixing analysis from small watersheds. Biogeochemistry. 2011; 105: 7–18. https://doi.org/10.1007/s10533-011-9597-8

114. Hayhoe SJ, Neill C, Porder S, Mchorney R, Lefebvre P, Coe MT, et al. Conversion to soy on the Amazonian agricultural frontier increases streamflow without affecting stormflow dynamics. Glob Chang Biol. 2011; 17: 1821–1833. https://doi.org/10.1111/j.1365-2486.2011.02392.x

115. Neill C, Germer S, Neto G, Krusche A, Chaves J, Neill C, et al. Land management impacts on runoff sources in small Amazon watersheds. Hydrol Process. 2008; 22: 1766–1775. https://doi.org/10.1002/hyp.6803

116. Coe MT, Costa MH, Soares-Filho BS. The influence of historical and potential future deforestation on the stream flow of the Amazon River–Land surface processes and atmospheric feedbacks. J Hydrol. 2009; 369: 165–174. https://doi.org/10.1016/j.jhydrol.2009.02.043

117. Bruijnzeel LA. Hydrological functions of tropical forests: Not seeing the soil for the trees? Agriculture, Ecosystems and Environment. 2004. https://doi.org/10.1016/j.agee.2004.01.015

118. Oliveira RS, Bezerra L, Davidson E a., Pinto F, Klink C a., Nepstad DC, et al. Deep root function in soil water dynamics in cerrado savannas of central Brazil. Funct Ecol. 2005; 19: 574–581. https://doi.org/10.1111/j.1365-2435.2005.01003.x